



ISSN: 0975-833X

## RESEARCH ARTICLE

### KINETIC AND THERMODYNAMIC ADSORPTION STUDY OF MILD STEEL CORROSION AND INHIBITION OF *AZADIRACHTA INDICA* GUM IN HYDROCHLORIC ACID SOLUTION

<sup>1</sup>Brindha, T. <sup>2</sup>Malarvizhi, M. and <sup>\*1</sup>Mallika, J.

<sup>1</sup>Department of Chemistry, PSG College of Arts and Science, Coimbatore 641014, India

<sup>2</sup>Department of Chemistry, Sri GVG Visalakshi College for Women, Udumalpet-642128, India

#### ARTICLE INFO

##### Article History:

Received 20<sup>th</sup> June, 2015

Received in revised form

30<sup>th</sup> July, 2015

Accepted 10<sup>th</sup> August, 2015

Published online 30<sup>th</sup> September, 2015

##### Key words:

Corrosion inhibition,  
Hydrochloric acid solution,  
Mild steel, FT-IR

Copyright © 2015 Brindha et al. This is an open access article distributed under the Creative Commons Attribution License, which permits unrestricted use, distribution, and reproduction in any medium, provided the original work is properly cited.

**Citation:** Brindha, T., Malarvizhi, M. and Mallika, J. 2015. "Kinetic and thermodynamic adsorption study of mild steel corrosion and inhibition of *Azadirachta Indica* gum in hydrochloric acid solution", *International Journal of Current Research*, 7, (9), 20510-20518.

#### ABSTRACT

The inhibition action of *Azadirachta indica* gum was tested as corrosion inhibitor for mild steel in 1 mol L<sup>-1</sup> HCl using weight loss and electrochemical techniques. Results show that the inhibition efficiency increases with decreasing temperature and increasing inhibitors concentration. The effect of temperature (303 - 328±1 K) on the inhibition of corrosion have also been studied. Corrosion kinetic parameters and thermodynamic adsorption parameters have been calculated and discussed in detail. The adsorption of this gum on the mild steel surface obeys Langmuir adsorption isotherm. The mechanism of inhibition process is established using FT-IR spectroscopy.

## INTRODUCTION

Natural gums are indispensable recipient in pharmaceutical, food and cosmetic industries (Anderson and Morrison, 1990). They are typically considered as any muggy substance that exudes from certain plants. It hardens on exposure to air and dissolves or forms glutinous oodles in water. In terms of solvent loving characteristics, gums are either hydrophobic or hydrophilic. They are colloids of high molecular weight molecules. Several studies have been carried out and reported for some plant gums and it is generally accepted that industrial utilization of a given gum depends on its physiochemical and rheological properties (Mothe and Rao, 1999). Natural guar gum is also employed as a binder of water-insoluble, ultrafine minerals in the froth flotation of potash ores (Ma and Pawlik, 2007). Some gums have also been found to be good corrosion inhibitors for the corrosion of metals in acidic solutions. According to Eddy *et al.*, (2011), gums have been found to be good corrosion inhibitors due to the following basis;

- Through their functional groups, they form complexes with metal ions and on the metal surfaces.
- Gum-metal complexes occupy a large surface area, thereby blanketing the surface and protecting the metals from corrosive agents present in the solution.
- The presence of arabinogalactan, sucrose, oligosaccharides, polysaccharides and glucoproteins since these compounds contain oxygen and nitrogen atoms which are the centers of adsorption.
- Natural gums are non-toxic, green and eco-friendly.

In view of the numerous advantages offered by some gums for corrosion inhibition systems, Umoren *et al.*, (2006) reported the potential of *Gum Arabic* as corrosion inhibitor for aluminium in alkaline medium. The effect of naturally occurring exudate gum from *Raphia hookeri* on the corrosion of mild steel in H<sub>2</sub>SO<sub>4</sub> in the temperature range 30-60 °C was also investigated by Umoren *et al.*, (2008) using weight loss and hydrogen evolution techniques. *Guar gum* has been shown to be an effective corrosion inhibitor for metal in aggressive acid environment by Abdallah (2004). The present work investigates the corrosion inhibition and thermodynamic adsorption study of gum exudates of *Azadirachta indica* (AI gum) on mild steel in 1 mol L<sup>-1</sup> HCl. The inhibition efficiency has been tested by weight

**\*Corresponding author: Mallika, J.**

Department of Chemistry, PSG College of Arts and Science,  
Coimbatore 641014, India.

loss, potentiodynamic polarization and electrochemical impedance spectroscopic methods. The effect of temperature (303- 328±1 K) and immersion time (1, 2, 3, 4, 5 and 24 h) on the corrosion behavior of mild steel was studied using weight loss measurements. The kinetic and thermodynamic adsorption studies for mild steel corrosion and inhibitor adsorption were determined and discussed in detail. The surface of the mild steel in the absence and presence of inhibitor has been analysed by employing FT-IR spectroscopy and scanning electron microscopy.

## MATERIALS AND METHODS

### Materials

The gum exudates of *Azadirachta indica* A. Juss. *Meliaceae* was collected locally and identified taxonomically and authenticated by the Botanical Survey of India (BSI), Coimbatore, Tamil Nadu, India. Laboratory grade hydrochloric acid solution was used as an aggressive medium. All the solutions were prepared using double distilled water. The mild steel of the composition 0.07 wt. % C, 0.008 wt. % P, 0.34 wt. % Mn, remaining iron (Fe) was used in the study. The metal specimens used for weight loss measurements were cut to obtain rectangular surfaces with dimensions of 25 x 10 x 1 mm with a hole drilled at the upper edge in order to hook it in the glass rod for immersion in the aggressive medium. Substantial layer of the specimen was removed by using various grades of abrasive papers and degreased by scrubbing with bleach- free scouring powder, followed by thorough rinsing in water and acetone.

### Methods

The gravimetric experiments were carried out according to the ASTM practice standard G-31 (ASTM International, 2004). Before initiating the experiments, the pre-cleaned specimens were weighed on a balance using 0.1 mg precision. The weighed specimens were immersed in the corrosive medium with and without inhibitors for 1 hour. After the experiment, the specimens were removed from the corrosive medium and immersed in the Clark solution for 40 seconds, rinsed with water, cleaned with acetone, dried in hot air and finally weighed. The mean of weight loss values of three identical specimens were used to calculate the corrosion rate and inhibition efficiency of the inhibitor. Corrosion rate and inhibition efficiency were calculated using the formulae given in equation (1) and (2)

$$\text{Corrosion rate (mmpy)} = 87.6 \times \frac{W}{\rho A t} \quad \dots\dots\dots(1)$$

where, W is the weight loss (g), 'ρ' the density of the mild steel specimen (g cm<sup>-3</sup>), 'A' the area of specimen (cm<sup>2</sup>) and t is the time of exposure (h).

$$\text{Inhibition efficiency (\%)} = \frac{W_o - W_i}{W_o} \times 100 \quad \dots\dots\dots(2)$$

$$\theta = 1 - \frac{W_i}{W_o} \quad \dots\dots\dots(3)$$

where, W<sub>i</sub> and W<sub>o</sub> are the weight losses of mild steel in inhibited and uninhibited solution respectively.

The electrochemical experiments were performed using three-electrode cell assembly. The cell consisted of a platinum counter electrode and a saturated calomel electrode (SCE) as the reference electrode. The working electrode was immersed in the acid solution and the constant steady-state (open circuit) potential was recorded as a function of time, when it became virtually constant. The polarization studies were carried out over a potential of +200 to -200 mV with respect to the open circuit potential at a scan rate of 1 mV s<sup>-1</sup>. The linear Tafel segments of the cathodic curves and the calculated anodic Tafel lines were extrapolated to the point of intersection to obtain the corrosion potential (E<sub>corr</sub>) and corrosion current density (i<sub>corr</sub>). The inhibition efficiency was evaluated from the measured I<sub>corr</sub> values using equation (4)

$$\text{Inhibition efficiency (\%)} = \frac{i_{\text{corr}}^o - i_{\text{corr}}}{i_{\text{corr}}} \times 100 \quad \dots\dots\dots(4)$$

where, i<sub>corr</sub><sup>o</sup> is the corrosion current density without inhibitor and i<sub>corr</sub> is the corrosion current density with inhibitor.

The electrochemical impedance spectroscopic (EIS) measurements were carried out using AC signals of 10 mV amplitude over the frequency range of 10 KHz to 0.01 Hz. The electrode was immersed in the solution for half an hour before starting the impedance measurements. All the impedance data were automatically controlled by Z<sub>view</sub> software and the diagrams were given as Nyquist plots. The charge transfer resistance (R<sub>ct</sub>) values were obtained from the diameter of the semicircles of the Nyquist plots. The inhibition efficiency of the inhibitor has been found out from the charge transfer resistance values according to the following equation (5)

$$\text{Inhibition efficiency (\%)} = \frac{R_{\text{ct}} - R_{\text{ct}}^o}{R_{\text{ct}}} \times 100 \quad \dots\dots\dots(5)$$

where, R<sub>ct</sub> and R<sub>ct</sub><sup>o</sup> are the charge transfer resistance with and without inhibitors respectively.

To determine the interaction of inhibitors with the mild steel specimen, a Shimadzu FT-IR 8000 spectrophotometer is employed in the 4000-400 cm<sup>-1</sup> region with KBr disc technique.

## RESULTS AND DISCUSSION

### Effect of inhibitor concentration

The corrosion of mild steel in 1 mol L<sup>-1</sup> HCl in the absence and presence of various concentrations (2 – 20 × 10<sup>-3</sup>g L<sup>-1</sup>) of AI gum was investigated at 303±1 K using weight loss measurements for 1 hour immersion period. Corrosion rate (mmpy), inhibition efficiency (%) and surface coverage (θ) were calculated using the equations

(1), (2) and (3) and the results are given in Table 1. Analysis of Table 1 indicates that the corrosion rate of AI gum gradually increases with increase in the concentration. The rate of corrosion on the mild steel surface in the presence of AI gum was found to be dependent upto  $60 \times 10^{-3} \text{ g L}^{-1}$  concentration of AI gum. Beyond this concentration, there is no appreciable change in the inhibiting performance of AI gum, indicating the attainment of limiting value.

**Table 1. Corrosion parameters for various concentrations of AI gum on mild steel in 1 mol L<sup>-1</sup> HCl**

Concentration ( $\times 10^{-3} \text{ g L}^{-1}$ )	Inhibition efficiency (%)	Corrosion rate (mmpy)	Surface coverage ( $\theta$ )
Blank	-	0.025	-
2	10.1	0.032	0.101
4	23.8	0.028	0.238
6	44.2	0.018	0.442
8	45.6	0.020	0.456
10	49.7	0.019	0.497
20	67.9	0.0090	0.679
40	70.0	0.0081	0.700
60	73.5	0.0071	0.735
80	73.2	0.0073	0.732

The increased inhibition efficiency with increasing AI gum concentration indicates that more gum molecules are adsorbed on the steel surface leading to the formation of protective film (Rao and Singhal, 2009). This behavior could be attributed to the increase of the surface coverage by the adsorption of inhibitor on the mild steel surface, which trims down the contact between the mild steel surface and acidic medium, thereby reducing the corrosion process (Mobin *et al.*, 2011). The adsorption of AI gum may be attributed due to the interaction between the lone pair of electrons of oxygen atom and the vacant d orbitals of the mild steel surface. However, the presence of chloride ions in the inhibited acid solution play a significant role in the adsorption process that results from increased surface coverage as a result of ion-pair interactions between the organic cations and the chloride ions (Abu-Dalo, 2012). An additional prospect may be due to the formation of positively charged glucoproteins of the AI gum in acidic solution, which smooths the progress of adsorption on the mild steel surface through a coordinate type of linkage.

**Effect of Temperature**

It is well known that temperature has a profound effect not only on corrosion rates, but also influences the inhibitor requirements because it affects inhibitor stability and solubility. Analysis of the temperature dependence of inhibition efficiency in absence and presence of inhibitor gives some insight into the possible mechanism of inhibitor adsorption.

The effect of temperature on the corrosion inhibition performance of selected concentrations ( $20 - 60 \times 10^{-3} \text{ g L}^{-1}$ ) of AI gum on mild steel in 1 mol L<sup>-1</sup> HCl was investigated by weight loss measurements in the temperature range of 303 - 328±1 K. Table 2 shows the calculated values of corrosion rate, inhibition efficiency and surface coverage for the AI gum. Analysis of table suggests that AI gum is adsorbed on the mild steel surface at the temperature range studied. It was noted that the corrosion rate is less in the presence of AI gum compared to free acid solution. A decrease in inhibition efficiency with increasing temperature proposes probable desorption of some of the adsorbed AI gum from the mild steel surface.

This behavior is suggestive of physical adsorption mechanism may be attributed to increase in the solubility of the protective films and any reaction products precipitated on the surface of the mild steel which inhibit the corrosion process. This is due to the fact that the quantity of equilibrium of adsorption decreases as temperature increases. Thus, as the temperature increases, the number of adsorbed molecules decreases, leading to decrease in the inhibition efficiency. It has been postulated that inhibitors reduce the corrosion processes by (Obot *et al.*, 2009),

- increasing the anodic or cathodic polarization behavior,
- reducing the movement or diffusion of ions to the metallic surface, and
- increasing the electrical resistance of the metallic surface.

Both anodic and cathodic effects are sometimes observed in the presence of natural polysaccharides.

**Corrosion kinetic parameters**

To evaluate the adsorption of the AI gum and to compute the activation parameters, the activation kinetic analysis is opted. The activation energy ( $E_a^*$ ) for the corrosion process, Arrhenius equation is used which is given in the equation (6)

$$\log CR = \log A - \frac{E_a^*}{2.303RT} \dots\dots\dots(6)$$

where,  $E_a^*$  is the apparent activation energy, R is the universal gas constant, T is the absolute temperature and A is the frequency factor. The relationship among temperature, inhibition efficiency and the activation energy of an inhibitor is given as follows (Ma and Pawlik, 2007). A decrease in inhibition efficiency with the rise in temperature with analogous increase in corrosion activation energy in the presence of inhibitor compared to its absence is frequently interpreted as being suggestive of formation of an adsorption film of physical (electrostatic) nature.

**Table 2. Corrosion parameters for selected concentrations of AI gum on mild steel in 1 mol L<sup>-1</sup> HCl at different temperatures**

Concentration ( $\times 10^{-3} \text{ g L}^{-1}$ )	Inhibition efficiency (%)			Corrosion rate (mmpy)			Surface coverage ( $\theta$ )		
	303 ± 1 K	318 ± 1 K	328 ± 1 K	303 ± 1 K	318 ± 1 K	328 ± 1 K	303 ± 1 K	318 ± 1 K	328 ± 1 K
20	67.9	56.4	42.6	0.0090	0.024	0.075	0.679	0.564	0.426
40	70.0	62.3	58.6	0.0081	0.021	0.054	0.700	0.623	0.586
60	73.5	65.5	58.7	0.0071	0.019	0.054	0.735	0.655	0.587
80	73.2	64.4	57.1	0.0073	0.020	0.058	0.732	0.644	0.571

The reverse effect, corresponding to an increase in inhibition efficiency with rise in temperature and lower activation energy in the presence of inhibitor, suggests a chemisorption mechanism.

unity for all the systems studied. The calculated values of apparent activation energy are given in Table 3.

**Table 3. Corrosion kinetic parameters for mild steel in 1 mol L<sup>-1</sup> HCl in absence and presence of different concentrations AI gum**

Concentration ( $\times 10^{-3}$ g L <sup>-1</sup> )	E <sub>a</sub> <sup>*</sup> (kJ mol <sup>-1</sup> )	$\Delta H^{\ddagger}$ (kJ mol <sup>-1</sup> )	E <sub>a</sub> <sup>*</sup> - $\Delta H^{\ddagger}$ (kJ mol <sup>-1</sup> )	$\Delta S^{\ddagger}$ (J mol <sup>-1</sup> )
Blank	50.5	47.9	2.6	-117.3
20	68.4	65.8	2.6	-67.5
40	61.9	59.4	2.5	-89.4
60	65.8	63.2	2.6	-77.8
80	67.0	64.4	2.6	-77.8

**Table 4. Thermodynamic adsorption parameters for the AI gum on mild steel in 1mol L<sup>-1</sup>HCl at different temperatures**

Temperature ( $\pm 1$ K)	Intercept	K (M <sup>-1</sup> )	$\Delta G_{\text{ads}}^{\circ}$ (kJ mol <sup>-1</sup> )	$\Delta H_{\text{ads}}^{\circ}$ (kJ mol <sup>-1</sup> )	$\Delta S_{\text{ads}}^{\circ}$ (J K <sup>-1</sup> mol <sup>-1</sup> )
303	0.0034	294.11	25.0		
318	0.0237	42.14	21.2	-86.27	-204.85
328	0.0437	22.88	19.5		

**Table 5. Potentiodynamic polarization parameters for the corrosion inhibition of mild steel in 1mol L<sup>-1</sup> HCl with and without inhibitors**

Concentration ( $\times 10^{-3}$ g L <sup>-1</sup> )	i <sub>corr</sub> / (mAcm <sup>-2</sup> )	E <sub>corr</sub> / (mV/SCE)	b <sub>a</sub> / (mVdec <sup>-1</sup> )	b <sub>c</sub> / (mVdec <sup>-1</sup> )	Inhibition efficiency /%
Blank	1.21	-499.38	94.4	137.2	-
20	1.08	- 503.2	79	124	10.5
40	0.595	-486.9	72	110	71.4
80	0.138	- 501.3	73	118	57.9

**Table 6. AC Impedance parameters for mild steel in 1mol L<sup>-1</sup>HCl containing AI gum**

Concentration ( $\times 10^{-3}$ g L <sup>-1</sup> )	R <sub>ct</sub> ( $\Omega$ cm <sup>2</sup> )	C <sub>dl</sub> ( $\mu$ Fcm <sup>-2</sup> ) $\times 10^{-3}$	Inhibition efficiency (%)
Blank	9.2	0.0046	-
20	12.5	0.0025	25.9
40	14.8	0.0018	37.8
80	51.4	0.0008	51.2

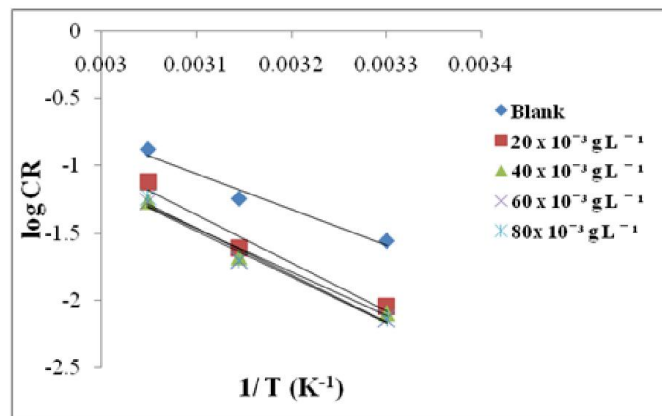


**Fig.1. Arrhenius plots for AI gum on mild steel in 1 mol L<sup>-1</sup> HCl: (a) blank; (b) 20  $\times 10^{-3}$  g L<sup>-1</sup>; (c) 40  $\times 10^{-3}$  g L<sup>-1</sup>; (d) 60  $\times 10^{-3}$  g L<sup>-1</sup>; (e) 80  $\times 10^{-3}$  g L<sup>-1</sup>**

The apparent activation energy for AI gum was determined by the linear regression between log CR and 1/T and the represented plots are given in Figure 1. Plots of log CR versus 1/T gave straight line with slope (-E<sub>a</sub><sup>\*</sup>/2.303R) and intercept A. The linear regression coefficients were close to

Other kinetics data (enthalpy and entropy of corrosion process) are accessible using the alternative formulation of the Arrhenius equation

$$CR = \left(\frac{RT}{Nh}\right) \exp\left(\frac{\Delta S^{\ddagger}}{R}\right) \exp\left(\frac{-\Delta H^{\ddagger}}{RT}\right) \dots\dots\dots(7)$$

where,  $h$  is Planck's constant,  $N$  the Avogadro's number,  $R$  is the universal gas constant,  $T$  the absolute temperature,  $\Delta S^*$  the entropy of activation and  $\Delta H^*$  the enthalpy of activation. Figure 2 shows the straight line plot of  $\log (CR/T)$  versus  $1/T$  gives straight line with slope  $(-\Delta H^*/ 2.303 R)$  and an intercept  $(\log (R/ Nh) + \Delta S^*/ 2.303 R)$ , from which  $\Delta H^*$  and  $\Delta S^*$  are calculated and included in Table 3.

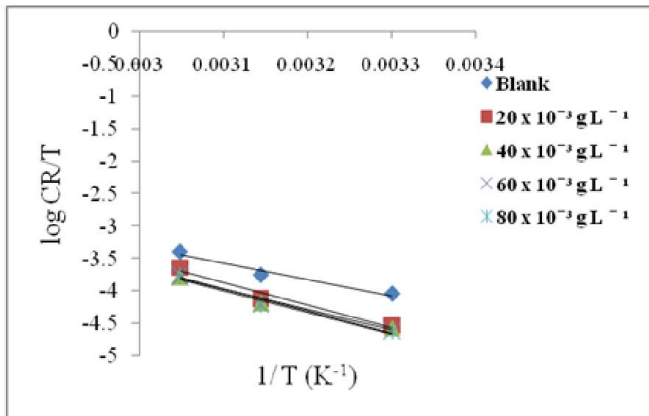


Fig. 2. Transition state plots for AI gum on mild steel in 1 mol L<sup>-1</sup> HCl: (a) blank; (b) 20 × 10<sup>-3</sup> g L<sup>-1</sup>; (c) 40 × 10<sup>-3</sup> g L<sup>-1</sup>; (d) 60 × 10<sup>-3</sup> g L<sup>-1</sup>; (e) 80 × 10<sup>-3</sup> g L<sup>-1</sup>.

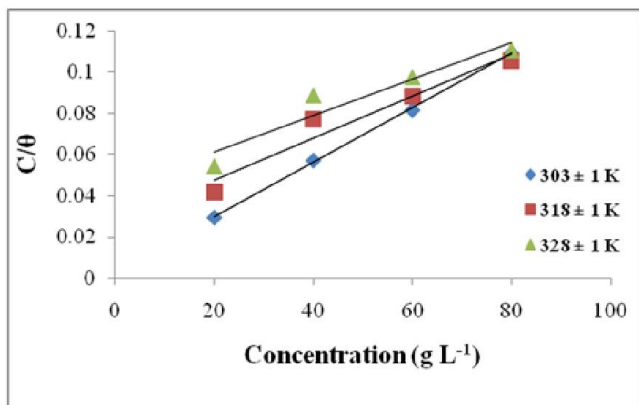


Fig. 3. Langmuir isotherm for the adsorption of AI gum on the mild steel surface in 1 mol L<sup>-1</sup> HCl at different temperatures

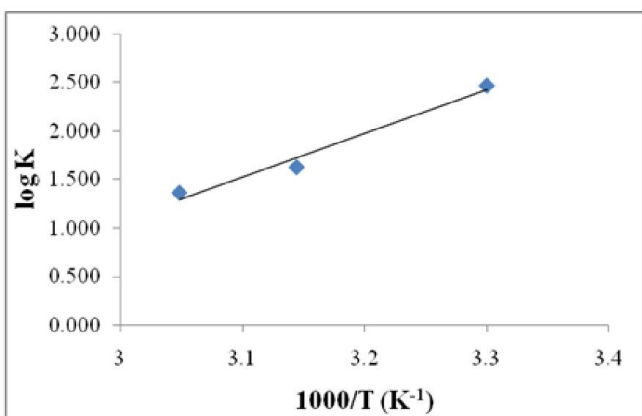


Fig. 4. Dependence of log K on 1/T for AI gum on mild steel in 1 mol L<sup>-1</sup> HCl

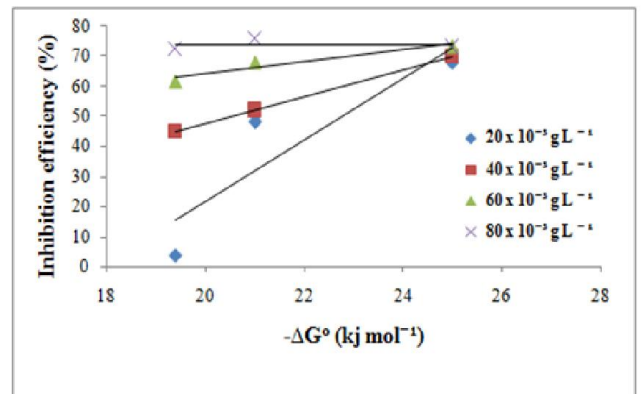


Fig.5. Dependence of inhibition efficiency of the AI gum on  $\Delta G_{ads}^0$  at different temperatures

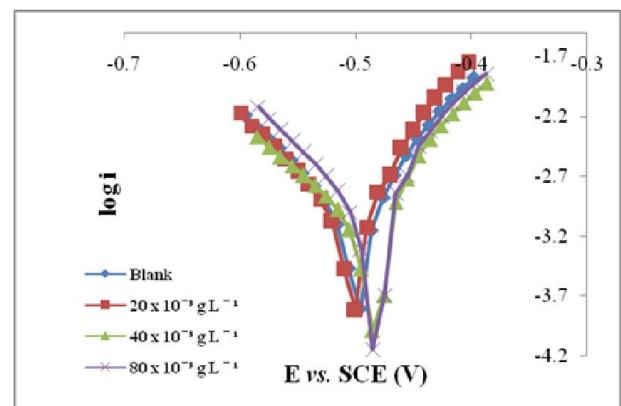


Fig.6. Potentiodynamic polarization curves for mild steel in 1 mol L<sup>-1</sup> HCl in the presence of various concentrations of AI gum

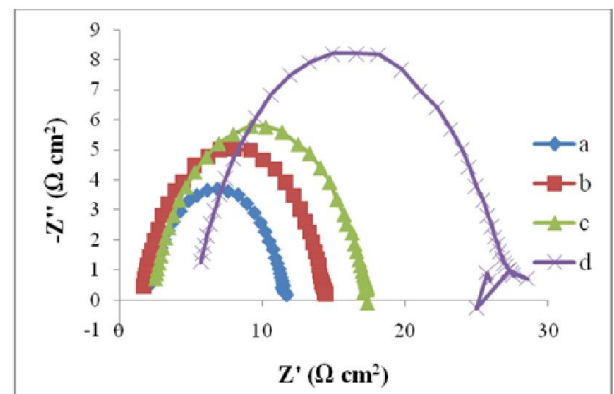


Fig.7. Nyquist plots of mild steel in 1 mol L<sup>-1</sup> HCl: (a) blank; (b) 20 × 10<sup>-3</sup> g L<sup>-1</sup> AI gum; (c) 40 × 10<sup>-3</sup> g L<sup>-1</sup> AI gum; (d) 80 × 10<sup>-3</sup> g L<sup>-1</sup> AI gum

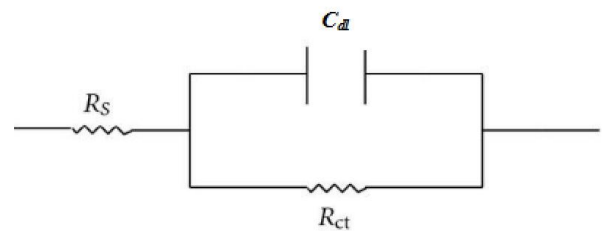


Fig. 8. The equivalent circuit model used to fit the EIS experiment data for mild steel in 1 mol L<sup>-1</sup> HCl

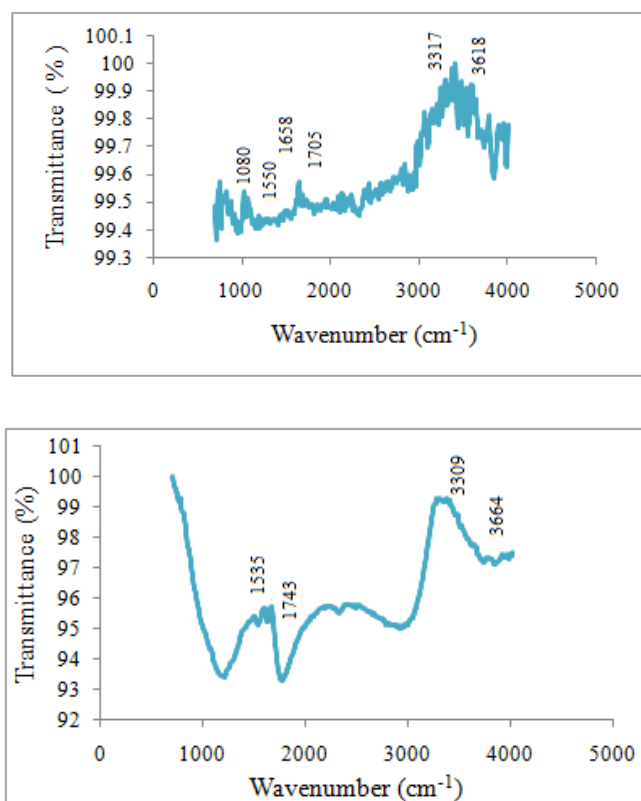


Fig. 9. (a) FT-IR spectrum of pure AI gum; (b) FT-IR spectrum of mild steel immersed in 1 mol L<sup>-1</sup> HCl in the presence of AI gum

All the calculated corrosion kinetic parameters ( $E_a^*$ ,  $\Delta H^*$  and  $\Delta S^*$ ) are analysed and the results are interpreted as follows:

- The value of  $E_a^*$  determined in 1 mol L<sup>-1</sup> HCl (blank) solution was 50.5 kJ mol<sup>-1</sup>.  $E_a^*$  for the inhibited system increases with increases in the concentration until it reaches a minimum value at concentration of  $80 \times 10^{-3}$  g L<sup>-1</sup> for AI gum. It is clear that activation energies for the inhibited solution are higher than the blank. The higher value of the  $E_a^*$  of the process in an inhibitor's presence when compared to that in its absence is attributed to its physisorption (Umoren and Ebenso, 2009). This indicates a strong inhibitive action for the studied compounds by increasing the energy barrier for the corrosion process, emphasizing the electrostatic character of the inhibitor's adsorption on mild steel surface. The values of activation energy for AI gum at four different concentrations ( $20, 40, 60$  and  $80 \times 10^{-3}$  g L<sup>-1</sup>) are 61.4, 61.9, 64.7 and 67.0 kJ mol<sup>-1</sup> respectively.
- The change in enthalpy ( $\Delta H^*$ ) for the inhibited solution containing various concentrations of AI gum are higher than the blank again supports the physical mode of adsorption. Also, the positive values of  $\Delta H^*$  in the uninhibited and inhibited solutions reflects the endothermic nature of mild steel dissolution.
- As observed from the Table 4, for all the concentrations  $E_a^* > \Delta H^*$  by a value which is exactly equal to RT. From the thermodynamic and kinetic point of view,

the unimolecular reactions are characterized by the following equation (Laidler, 1963) (7)

$$E_a^* - \Delta H^* = RT \dots\dots\dots(7)$$

Hence, mild steel specimen corrodes in 1 mol L<sup>-1</sup> HCl in both the uninhibited and inhibited solutions by a unimolecular reaction.

- The values of  $\Delta S^*$  for the uninhibited solution was -117.3 J K<sup>-1</sup> mol<sup>-1</sup> and it increases towards more negative side in increase in concentration of AI gum upto maximum of -147.5 J K<sup>-1</sup> mol<sup>-1</sup>. The negative values for  $\Delta S^*$  in the inhibited and uninhibited systems implies that the activation complex in the rate determining step represents association rather than dissociation step, meaning that a decrease in disorder takes place on going from reactant to the activated complex (Abd El-Rehim, 2001).

**Thermodynamic adsorption parameters**

Adsorption isotherms provide information about the interaction among the adsorbed molecules themselves and also their interactions with the electrode surface. Adsorption of AI gum on the mild steel surface was tested graphically by fitting to various adsorption isotherm.

$$\frac{C}{\theta} = \frac{1}{K} + C \dots\dots\dots(8)$$

where,  $\theta$  is the degree of surface coverage, C is the concentration, and K is the equilibrium constant for the process of adsorption. The  $\theta$  values have been calculated from the weight loss measurements.

Figure 3 show the linear fitting of AI gum on mild steel surface in 1 mol L<sup>-1</sup> HCl solution. The best fit was obtained with the Langmuir isotherm. From the intercept of the Langmuir plots, K values are obtained and given in Table 4. The equilibrium constant of adsorption K is related to the standard free energy of adsorption ( $\Delta G_{ads}^o$ ) by:

$$K = -\log C_{H_2O} - \left( \frac{\Delta G_{ads}^o}{2.303 RT} \right) \dots\dots\dots(9)$$

where,  $C_{H_2O}$  is the molar concentration of water molecules at the electrode/electrolyte interface.

Thermodynamically,  $\Delta G_{ads}^o$  is related to the enthalpy and entropy of adsorption process,  $\Delta H_{ads}^o$  and  $\Delta S_{ads}^o$  respectively, by the equation (10)

$$\Delta G_{ads}^o = \Delta H_{ads}^o - T\Delta S_{ads}^o \dots\dots\dots(10)$$

By rearranging the equations (9) and (10) the following equation can be written according to Noor et al., 2008.

$$\log K = (-\log C_{\text{H}_2\text{O}} + \frac{\Delta S_{\text{ads}}^{\circ}}{2.303R}) - \frac{\Delta H_{\text{ads}}^{\circ}}{2.303RT} \quad \dots\dots\dots(11)$$

A plot of  $\log K$  vs.  $1/T$  gives straight lines as shown in Figure 4. The slope of this line is  $\Delta H_{\text{ads}}^{\circ}/2.303R$  and the intercept is  $(-\log C_{\text{H}_2\text{O}} + \Delta S_{\text{ads}}^{\circ}/2.303R)$ , from which the values of  $\Delta H_{\text{ads}}^{\circ}$  and  $\Delta S_{\text{ads}}^{\circ}$  were calculated, respectively. The calculated values are included in Table 5.

The estimated values of  $K$ ,  $\Delta G_{\text{ads}}^{\circ}$ ,  $\Delta H_{\text{ads}}^{\circ}$  and  $\Delta S_{\text{ads}}^{\circ}$  are provided in Table 5 and the following interpretations can be made:

- Large values of  $K$  indicate that there is a strong interaction between the phase boundaries of double layer and the adsorbed inhibitor, which results in better inhibition efficiency.
- The negative values of  $\Delta G_{\text{ads}}^{\circ}$  indicates that the adsorption of AI gum on the mild steel surface is spontaneous. This behavior is correlated with Figure 5, showing the relationship between inhibition efficiency of AI gum and their  $\Delta G_{\text{ads}}^{\circ}$  values at different temperatures. It can be seen from Figure 5, that adsorption of AI gum obey the general rule that inhibition efficiency increases with increase in negative value of  $\Delta G_{\text{ads}}^{\circ}$ .
- Generally, values of  $\Delta G_{\text{ads}}^{\circ}$ , around  $-20 \text{ kJ mol}^{-1}$  or lower are consistent with the electrostatic interaction between charged molecules and the charged metal surface (physisorption); those around  $-40 \text{ kJ mol}^{-1}$  or higher involve charge sharing or transfer from organic molecules to the metal surface to form a coordinate type of metal bond (chemisorption). The calculated values of  $\Delta G_{\text{ads}}^{\circ}$  at 303 and  $318 \pm 1 \text{ K}$  are slightly greater than  $-20 \text{ kJ mol}^{-1}$ , indicating that the adsorption is not merely physisorption or chemisorption but obeying a comprehensive adsorption (physical and chemical adsorption).
- It also noted that there is a limited decrease in the value of  $\Delta G_{\text{ads}}^{\circ}$ , which implies that the adsorption was unfavorable under the studied temperature range, shows that physisorption has the major contribution while chemisorption has the minor contribution in the adsorption mechanism.
- The obtained negative value of  $\Delta H_{\text{ads}}^{\circ}$  reflects that the adsorption of AI gum onto the mild steel surface is an exothermic process. Exothermic process differentiate the physisorption and chemisorption by considering the value of  $\Delta H_{\text{ads}}^{\circ}$ . In general the  $\Delta H_{\text{ads}}^{\circ}$  values lies below  $-40 \text{ kJ mol}^{-1}$  attributes to physisorption and that of  $-100 \text{ kJ mol}^{-1}$  is chemisorption. In this present work, the  $\Delta H_{\text{ads}}^{\circ}$  values are higher than common physical adsorption of heat, but lower than common chemical adsorption of heat, again accentuating the

nature of comprehensive adsorption taken place by AI gum. The obtained negative values of  $\Delta S_{\text{ads}}^{\circ}$  implies that ordered progress in adsorption of AI gum onto the mild steel surface.

### Potentiodynamic polarization measurements

Polarization curves for mild steel in  $1 \text{ mol L}^{-1}$  HCl solutions at room temperature without and with addition of different concentrations of AIG are shown in Figure 6. The anodic and cathodic current potential curves are extrapolated up to their intersection at the point where corrosion current density ( $i_{\text{corr}}$ ) and corrosion potential ( $E_{\text{corr}}$ ) are obtained. The electrochemical parameters  $i_{\text{corr}}$ ,  $E_{\text{corr}}$ , anodic, and cathodic Tafel slopes ( $b_a$  and  $b_c$ ) obtained from polarization measurement are listed in Table 5.

It was observed from the table that the addition of  $20 \times 10^{-3} \text{ g L}^{-1}$  AI gum to the corrosive medium shows higher value of  $E_{\text{corr}}$  than the free acid solution. However, it exhibited a lower value of  $E_{\text{corr}}$  for additives of 40 and  $80 \times 10^{-3} \text{ g L}^{-1}$  AI gum. For example, the mild steel in corrosive medium containing  $20 \times 10^{-3} \text{ g L}^{-1}$  AI gum displayed high corrosion potential of  $-503.29 \text{ mV}$ . On increasing the concentration of AI gum by 50%, the corrosion potential shifted towards lower side of  $-486.34 \text{ mV}$ . Further increase in concentration, the potential remained at  $-486.35 \text{ mV}$ . Such  $E_{\text{corr}}$  values imply that the AI gum inhibited mild steel corrosion. In general, the changes observed in the polarization curves after addition of the inhibitor are usually used as criteria to classify inhibitors as cathodic, anodic or mixed (Eddy and Ebenso, 2008). From the figure, it can be seen that the corrosion potential for the addition of  $20 \times 10^{-3} \text{ g L}^{-1}$  AI gum shows slight shift in negative direction whereas in the case of 40 and  $80 \times 10^{-3} \text{ g L}^{-1}$  it shifted towards positive direction and to lower current densities. These results indicate that AI gum act as a mixed-type corrosion inhibitor with predominantly controlled of anodic reaction (Bouyanzer and Hammouti, 2004; Noor, 2007). This means that the AI gum have significant effects on retarding both the anodic dissolution of mild steel and inhibiting the cathodic hydrogen evolution. It can be also been observed from the table that AI gum has significant influence on both the anodic and cathode Tafel slopes, indicates that the inhibitor may change both the mechanism of cathodic reaction and anodic dissolution. The percentages of inhibition efficiency obtained are comparable with those calculated from weight-loss measurement. But some difference was observed and this could be attributed to the fact that the weight loss method gives average corrosion rates, whereas the polarization method gives instantaneous corrosion rates (Muralidharan *et al.*, 1995)

### Electrochemical impedance spectroscopy studies

Impedance measurements provide information on both the resistive and capacitive behaviour of the interface, evaluation on the performance of studied compounds as possible corrosion inhibitor, and investigation of the corrosion inhibition processes. Measurements were undertaken to assess the impedance parameters of the mild steel in  $1 \text{ mol L}^{-1}$  HCl

in the presence of certain concentrations of AI gum. Representative Nyquist plot is given in Figure 7. The spectra obtained without and with inhibitor contain depressed semi-circle with the centre under the real axis whose size increases with the inhibitor concentration, indicating a charge transfer process mainly controlling the corrosion of mild-steel. Such a behaviour, characteristic for solid electrodes and often refer to a frequency dispersion, has been attributed to roughness and other in homogeneities of the solid surface (Juttner, 1990; Ramesh saliyan, 2008). It is observed that increasing the concentration of AI gum results in an increase in the size of the semi-circle in Figure 7. The impedance spectra for the Nyquist plots were analyzed by fitting to the equivalent circuit model shown in Figure 8.

The characteristic parameters associated to the impedance diagrams (charge transfer resistance ( $R_{ct}$ ) and double layer capacitance ( $C_{dl}$ ) and inhibition efficiency were calculated and given in Table 6. The value of  $R_{ct}$  is a measure of electron transfer across the surface and inversely proportional to corrosion rate. Double layer capacitance ( $C_{dl}$ ) was obtained from the impedance measurements by using equation (12)

$$C_{dl} = \frac{1}{2\pi f_{max} R_{ct}} \quad \dots\dots\dots(12)$$

where,  $f_{max}$  is the frequency value at which the imaginary component of the impedance is maximum.

Inspection of Table 7 clearly shows that the values of  $R_{ct}$  increases with increase in concentration of AI gum. On the other hand, the values of  $C_{dl}$  decreased with increase in concentration. This is due to the increase in the surface coverage by AI gum, which leads to an increase in the inhibition efficiency. The decrease in  $C_{dl}$  value may resulted due to the decrease in local dielectric constant and/or an increase in the thickness of the electric double layer, suggested that the AI gum gets adsorbed onto the mild steel surface. This is due to the gradual replacement of water molecules by the adsorption of the inhibitor molecules on the mild steel surface, decreases the extent of metal dissolution and hence it causes the change in  $C_{dl}$  values. Further the inhibition efficiency was calculated and it was found that the values are in good agreement with those obtained from the weight loss measurements.

### FT-IR spectra

An explanation of the mechanism of inhibition requires full understanding of the interaction between the inhibiting compound and the metal surface. Corrosion inhibition of mild steel in hydrochloric acid solution by inhibitors can be explained on the basis of molecular adsorption (Bentiss, 2002). The adsorption process is influenced by the chemical structures, distribution of charge in molecule, the nature and surface charge of metal, and the type of aggressive media (Bahrami, 2012). The mechanism of inhibition of AI gum on the mild steel surface is established using FT-IR spectroscopy.

FT-IR spectrum of pure AI gum has been recorded and the relative intensities of the vibrational peaks are compared (Figure 9 (a)). As can be seen from the figure, the spectrum exhibits very clear and strong features assigned to the polysaccharide molecules in AI gum. It is characterized with its -OH characteristic stretching vibration frequency in the region between  $3317 \text{ cm}^{-1}$  -  $3618 \text{ cm}^{-1}$ . The bending mode of adsorbed water is seen (Andreeva et al., 2010) at  $1658 \text{ cm}^{-1}$ . The peak at  $1550 \text{ cm}^{-1}$  is assigned to the stretching vibrations of the carboxylate group. In order to address the adsorption of AI gum onto the mild steel surface, it is most useful to compare the relative intensities of the major vibrational modes of pure AI gum spectrum to those of AI gum ( $60 \times 10^{-3} \text{ g L}^{-1}$ ) after immersing in  $1 \text{ mol L}^{-1}$  HCl for 1 hour immersion period at  $303 \pm 1 \text{ K}$ . Figure 9 (b) represents the FT-IR spectrum of mild steel immersed in  $1 \text{ mol L}^{-1}$  HCl in the presence of AI gum. Close inspection of figure, reveals the presence of very interesting features. The major bands concerning the stretching vibrations of the O-H bond at  $3317\text{-}3618 \text{ cm}^{-1}$  and the stretching vibrations of the -C=O bond of carboxylate group associated with the AI gum at  $1550 \text{ cm}^{-1}$ , for which a decrease in intensity of  $1535 \text{ cm}^{-1}$  is observed in the Figure 9 (b). The peak for bending mode of  $\text{H}_2\text{O}$  molecule is also shifted towards lower wave numbers, which clearly indicates that the -OH group of AI gum molecules may form insoluble hydroxides on the surface of the mild steel, which leads to the reduction of corrosion rate by suppressing the cathodic hydrogen evolution reaction. The above shifting in the characteristic peaks can be attributed to the completely adsorbed polysaccharide molecules on the surface of steel in HCl. The overall features of the FT-IR spectrum suggested that there is a strong adsorption of AI gum onto the mild steel surface, due to the electrostatic binding of the carboxylate groups of the AI gum to sites along oxide surfaces of steel.

### Conclusion

AI gum is a very good corrosion inhibitor for mild steel in  $1 \text{ mol L}^{-1}$  HCl. The inhibition efficiency increases with increasing inhibitor concentration (upto  $60 \times 10^{-3} \text{ g L}^{-1}$ ) and decrease in temperature. First order type of reaction is obtained from the kinetic treatment of the data. The higher values of activation energy and enthalpy change in the inhibited medium supports physisorption. The adsorption of AI gum obeys the Langmuir adsorption isotherm at all investigated temperatures. Thermodynamic adsorption parameters ( $\Delta H_{ads}^{\circ}$ ,  $\Delta S_{ads}^{\circ}$  and  $\Delta G_{ads}^{\circ}$ ) show that the AI gum is adsorbed on mild steel surface by an exothermic, spontaneous process. According to  $\Delta H_{ads}^{\circ}$  value for the studied inhibitors, comprehensive (physisorption and chemisorption) adsorption is suggested to occur on mild steel surface. Polarization measurements showed the mixed-inhibition mechanism of the studied AI gum. The adsorbed film over the mild steel surface has been confirmed by SEM analysis. The mechanism of inhibition of mild steel corrosion by AI gum is well recognized by FT-IR spectroscopy.

## REFERENCES

- Abd El-Rehim, S.S., Hassan, H.H. and Amin, M.A. 2001. Corrosion inhibition of aluminum by 1,1 (lauryl amido) propyl ammonium chloride in HCl solution. *Materials Chemistry and Physics*, 70: 64-72.
- Abdallah, M. 2004. Guar Gum as Corrosion Inhibitor for Carbon Steel in Sulfuric Acid Solutions. *Electrochim. Acta.*, 22: 161-175.
- Abu-Dalo, M.A., Othman, A.A. and Al-Rawashdeh, N.A.F. 2012. Exudate Gum from Acacia Trees as Green Corrosion Inhibitor for Mild Steel in Acidic Media. *Int. J. Electrochem. Sci.*, 7: 9303-9324.
- Anderson, D.M.W. and Morrison, A. 1990. The identification of Cobretum gums which are not food additives. *Food Additives and Contaminants.*, 7: 175-180.
- Andreeva, D.V., Skorb, E.V., Shchukin, D.G. 2010. Layer-by-Layer Polyelectrolyte/Inhibitor Nanostructures for Metal Corrosion Protection. *Appl. Mater. Interfaces*, 2: 1954-1962.
- ASTM practice standard G-31 "Standard practice for laboratory immersion corrosion testing of metals", *ASTM International*, 2004.
- Bahrami, S.M. and Ali Hosseini, S.M. 2012. Electrochemical and thermodynamic investigation of the corrosion behavior of mild steel in 1 M hydrochloric acid solution containing organic compound. *Int. J. Indust. Chem.*, 30: 3-10.
- Bentiss, F., Lagrenee, M., Mehdi, B., Mernari, B., Traisnel, M. and Vezin, H. 2002. Electrochemical and quantum chemical studies of 3,5-di(n-tolyl)-4-amino-1,2,4-triazole adsorption on mild steel in acidic media. *Corros.*, 58: 399-407.
- Bouyanzer, A. and Hammouti, B. 2004. A study of anti-corrosive effects of Artemisia oil on steel. *Pigment. Res. Technol.*, 33: 287-292.
- Eddy, N.O. and Ebenso, E.E. 2008. Inhibitive and adsorption properties of Musa sapientum for the corrosion of mild steel in acid medium. *J. Pure. Appl. Chem.*, 2: 46-54.
- Eddy, N.O., Ameh, P., Gimba, C.E. and Ebenso, E.E. 2012. Corrosion Inhibition Potential of Daniella Oliverri Gum Exudate for Mild Steel in Acidic Medium. *Int. J. Electrochem. Sci.*, 7: 7425-7439.
- Juttner, K. 1990. Electrochemical impedance spectroscopy (EIS) of corrosion processes on inhomogeneous surfaces. *Electrochim. Acta.*, 35: 1501-1503.
- Laidler, K.J., 1963 Reaction Kinetics, Vol. 1, first ed., Pergamon Press, New York, 1963.
- Ma, X. and Pawlik, M. 2007. Role of Background Ions in Guar Gum Adsorption on Chloride Solutions. *Carbohydr. Polym.*, 70: 15-24.
- Mobin, M., Khan, M.A. and Parveen, M. 2011. Inhibition of Mild Steel Corrosion in Acidic Medium Using Starch and Surfactants Additives. *J. Appl. Poly. Sci.*, 121: 1558-1565.
- Mothe, C.G. and Rao, M.A. 1999. Rheological behaviour of aqueous dispersions of cashew gums and gum Arabic. *Food hydrocolloids*. 13: 501-506.
- Muralidharan, S., Quraishi, M.A. and Iyer, S.V.K. 1995. The effect of molecular structure on hydrogen permeation and the corrosion inhibition of mild steel in acidic solutions. *Corros. Sci.*, 37: 1739-175.
- Noor, E.A. and Al-Moubaraki, A.H. 2008. Thermodynamic study of metal corrosion and inhibitor adsorption processes in mild steel/1-methyl-4[4 (-X)-styryl pyridinium iodides/hydrochloric acid systems. *Mater. Chem. Phys.*, 110: 145-154.
- Obot, I.B., Obi-Egbedi, N.O. and Umoren, S.A. 2009. Adsorption characteristics and corrosion inhibitive properties of clotrimazole for aluminium corrosion in hydrochloric acid. *Int. J. Electrochem. Sci.*, 4: 863-877.
- Ramesh saliyam, V. and Airody vasudeva adhikari. 2008. Inhibition of corrosion of mild steel in acid media by N'-benzylidene-3-(quinolin-4-ylthio) propanohydrazide. *Bulletin. Mater. Sci.*, 31: 699-712.
- Rao, V.S. and Singhal, L.K. 2009. Corrosion behavior and passive film chemistry of 216L stainless steel in sulphuric acid. *J. Mater. Sci.*, 44: 2327-2333.
- Umoren, S.A. and Ebenso, E.E. 2008. Studies of the anti-corrosive effect of Raphia hookeri exudate gum-halide mixtures for aluminium corrosion in acidic medium. *Pigment. Res. Technol.*, 37: 173-182.
- Umoren, S.A. and Ebenso, E.E. 2007. The synergistic effect of polyacrylamide and iodide ions on the corrosion inhibition of mild steel in H<sub>2</sub>SO<sub>4</sub>. *Mater. Chem. Phys.*, 106: 387-393.
- Umoren, S.A., Obot, I.B., Ebenso, E.E., Okafor, P.C., Ogbobe, O. and Oguzie, E.E. 2006. Gum arabic as a potential corrosion inhibitor for aluminium in alkaline medium and its adsorption characteristics. *Anti-Corr. Meth. Mater.*, 53: 277-282.

\*\*\*\*\*